Non-Innocent Role of Sacrificial Anodes in Electrochemical Nickel-Catalyzed C(sp^2)-C(sp^3) Cross-Electrophile Coupling

Luana Cardinale[a], Gregory L. Beutner[b], Christopher Y. Bemis[b], Daniel J. Weix[a], and Shannon S. Stahl[a]*

[a]Department of Chemistry, University of Wisconsin-Madison, Madison, WI 53706, United States

[b]Bristol Myers Squibb, Chemical Process Development, 1 Squibb Drive, New Brunswick, NJ 08903, United States

ABSTRACT: Sacrificial anodes composed of inexpensive metals such as Zn, Fe and Mg are widely used to support electrochemical nickel-catalyzed cross-electrophile coupling (XEC) reactions, in addition to other reductive electrochemical transformations. Such anodes are appealing because they provide a stable counter-electrode potential and typically avoid interference with the reductive chemistry. The present study outlines development of an electrochemical Ni-catalyzed XEC reaction that streamlines access to a key pharmaceutical intermediate. Metal ions derived from sacrificial anode oxidation, however, directly contribute to homocoupling and proto-dehalogenation side products that are commonly formed in chemical and electrochemical Ni-catalyzed XEC reactions. Use of a divided cell limits interference by the anode-derived metal ions and supports high product yield with negligible side product formation, introducing a strategy to overcome one of the main limitations of Ni-catalyzed XEC.

Electrosynthetic reduction reactions encounter unique challenges relative to oxidation reactions. Whereas oxidations are often conducted "reagent-free", evolving H_2 at the counter electrode using electrons and protons derived from the substrate, reductions require an external source of electrons.[1–3] Sacrificial metal anodes are commonly used in these reactions because they can undergo facile oxidation at a controlled potential and avoid the need for chemical reductants, such as tertiary amines, that could interfere with the cathodic chemistry.[1–5] Electrochemical Ni-catalyzed cross-electrophile coupling (XEC) reactions are the focus of growing interest[6] because such methods avoid the constrained redox potentials[7] and complications associated with use Mn and Zn metal powder reductants.[8] Sacrificial anodes are widely used in these reactions. The first example in 1976 used an Al anode,[9] and other metals, including Fe, Zn, Mg, and stainless steel (SS), found use in subsequent studies.[10–20] Recent work at BMS revealed a strategic opportunity to use electrochemistry to prepare a pharmaceutical intermediate relevant to treatment of autoimmune disorders (**Figure 1A**).[21,22] Electrochemical Ni-catalyzed coupling of the piperidine and indole electrophiles **1b** and **2a** would streamline access to **3a**, replacing two Pd-catalyzed reactions in the current route with a single reaction using a non-precious-metal (Ni) catalyst [23,24] and a much lower cost piperidine-derived substrate (**Figure 1A**).[21] Preliminary studies, however, showed that Ni XEC routes to **3a** are complicated by homocoupling and/or proto-dehalogenation side products, reflecting a common challenge encountered in both chemical and electrochemical XEC reactions (**Figure 1B**). In the present study, analysis of electrochemical Ni-catalyzed XEC of **1b** and **2a** reveals that metal ions derived from sacrificial anodes are not innocent, but directly contribute to side product formation. Use of a divided electrochemical cell to restrict transport of these ions decreases or eliminates the side products. These results introduce an important strategy to improve selectivity in Ni-catalyzed XEC reactions.

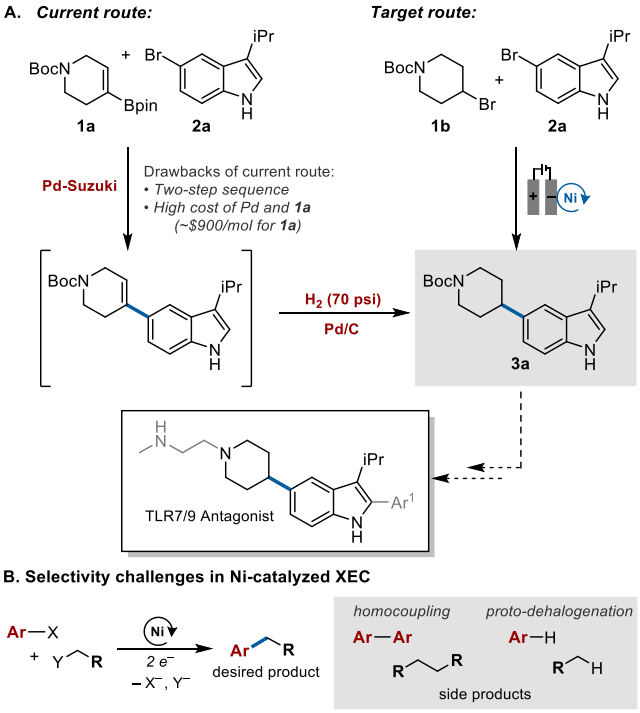

Figure 1. A) Comparison between the existing optimized conditions to synthesize **3a** and a streamlined electrochemical reaction that directly accesses **3a** from a lower cost piperidine substrate. B) Ni-catalyzed XEC reactions commonly form homocoupling and proto-dehalogenation side products.

The present study was initiated by employing the previously reported conditions: 5 mol% $NiBr_2$•(dtbbpy)$_2$ (dtbbpy = 4,4'-di-*tert*-butyl-2,2'-bipyridyl), **2a** and **1b** in a 1:1.5 ratio, and 0.2 M LiBr in *N*,*N*-dimethylacetamide (DMA) (**Figure 2A**). The electrolysis was performed in an undivided cell with an RVC (reticulated vitreous carbon) cathode and a sacrificial Zn anode. A constant current of –4 mA was applied, and the reaction

reached completion when ~2.1 F/mol of charge were passed with respect to **2a**. Under these conditions, **3a** was obtained in 71% yield, together with indole dimer **4a** (3% yield[25]) and proto-dehalogenated indole **5a** (28% yield) (**Figure 2B).** A time course of the reaction (**Figure 2B**) shows that side product formation exhibits an induction period, beginning with the appearance of **5a** at 0.9 F/mol and **4a** at 1.6 F/mol of charge passed, indicating that reaction selectivity drops as the reaction progresses.

The relatively poor reaction selectivity resembles observations made with Zn powder as a chemical reductant,[21] and raised the prospect that Zn^{2+} ions derived from sacrificial anodic oxidation could interfere with aryl-alkyl cross-coupling.[4,26–29] Therefore, we tested the same reaction in a divided electrolysis cell, with the anode and cathode compartments separated by a Nafion-115 cation exchange membrane (**Figure 2C**). We postulated the LiBr electrolyte could favor Li^+ ion transport through the membrane to balance charge during electrolysis and limit transport of Zn^{2+} ions into the cathode compartment. ICP-OES quantification of Zn shows that, indeed, no Zn is detected (<1 ppm) in the cathode of a divided cell when Zn is used as sacrificial anode (Supporting Information, **Figure S19**). Significantly improved yield and selectivity for product **3a** was observed when using this cell configuration: 92% yield of **3a** and < 1% yield of side products **4a** and **5a** (**Figure 2C**).[30]

Other sacrificial anode materials were then tested in the undivided cell configuration, including Fe, Mg, Al, and SS-304 (**Figure 2D**). Diisopropylethylamine (DIPEA) was also tested as a chemical reductant with an RVC anode.[31,32] These alternate anodes are generally inferior to Zn and show different selectivity profiles. Only the Al anode supports a yield similar to Zn. The Zn anode promotes formation of proto-dehalogenation side product **5a**, while Fe and SS-304 show enhanced formation of the biaryl homocoupling side product **4a** (**Figure 2D**). Often, both side products are observed. DIPEA shows poor substrate conversion, suggesting the amine or its degradation product inhibits catalytic turnover for this reaction.

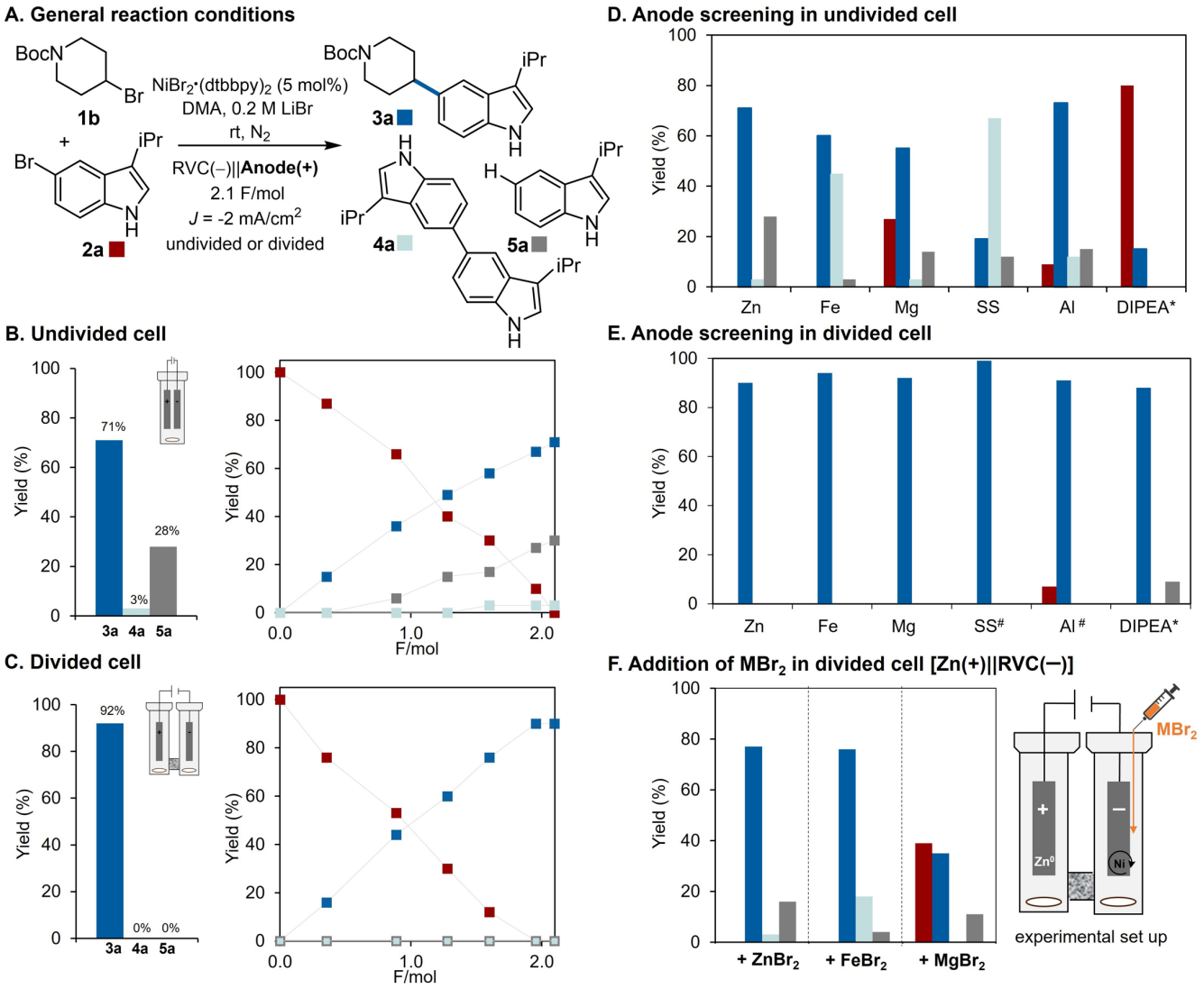

Figure 2. A) Previously optimized electrochemical conditions for the synthesis of **3a** from **2a** and **1b**[22] and its time course (B). C) Repeat of reaction in panel B, but with a divided cell containing a Nafion-115 membrane. ^{1}H NMR spectroscopic yields with 1,3,5-trimethoxybenzene as an external standard. D) Screening of various materials as anodes, undivided cell, reactions run on 0.42 mmol **2a** and 0.75 mmol **1b**; SS-304 = stainless steel; #reaction run with 0.4 M LiBr; *in the case of sacrificial DIPEA (*N*,*N*-diisopropylethylamine) the anode was a RVC electrode. E) Same reactions shown in (D) run in a divided cell, Nafion-115 separated. F) Addition of metal salts ($ZnBr_2$, $FeBr_2$, $MgBr_2$ respectively) into the cathode of reactions run in a divided cell (Nafion-115) with a Zn anode. Metals were dosed with a syringe pump (0.42 mmol MBr_2, 0.25 mL/h) with exception of $MgBr_2$ which was added from the beginning due to low solubility in DMA at high concentrations.

Significantly improved results were obtained with each of these anodes when using the divided cell (**Figure 2E**). No formation of side products **4a** or **5a** is observed when using Zn, Fe, or Mg. When using SS-304 or Al, small amounts of unconverted starting material **2a** and/or side products **4a** and **5a** are observed, possibly due to Al^{3+}, Ni^{2+} and Cr^{3+} cross-over into the cathode (Supporting Information, **Figure S6** and **Table S4**). However, higher concentrations of LiBr electrolytes can lower the diffusion of such ions and drastically improve selectivity (**Figure 2E**). Reactions run with DIPEA and an RVC anode showed formation of **5a**, likely resulting from facile cross-over of H^+ from the anode, where protons are generated from amine oxidation.[31] The influence of M^{2+} ions was further tested through control experiments, in which MBr_2 salts were slowly added via syringe pump to the cathode compartment in a divided cell to simulate the increasing concentration of these salts during electrolysis in an undivided cell (**Figure 2F**). The results align with observations obtained with the undivided cell experiments (cf. **Figure 2D**). Specifically, $ZnBr_2$ induces formation of proto-dehalogenation side product **5a**, $FeBr_2$[33] promotes formation of biaryl **4a**, and $MgBr_2$ both inhibits substrate conversion and promotes formation of **5a**. Collectively, these results show that sacrificial metal anodes are not innocent and can have a deleterious impact on Ni-catalyzed XEC reactions.

Zn and Fe are the most common sacrificial anodes used to support electrochemical Ni-catalyzed XEC reactions (**Figure S26** in the Supporting Information documents the frequency of

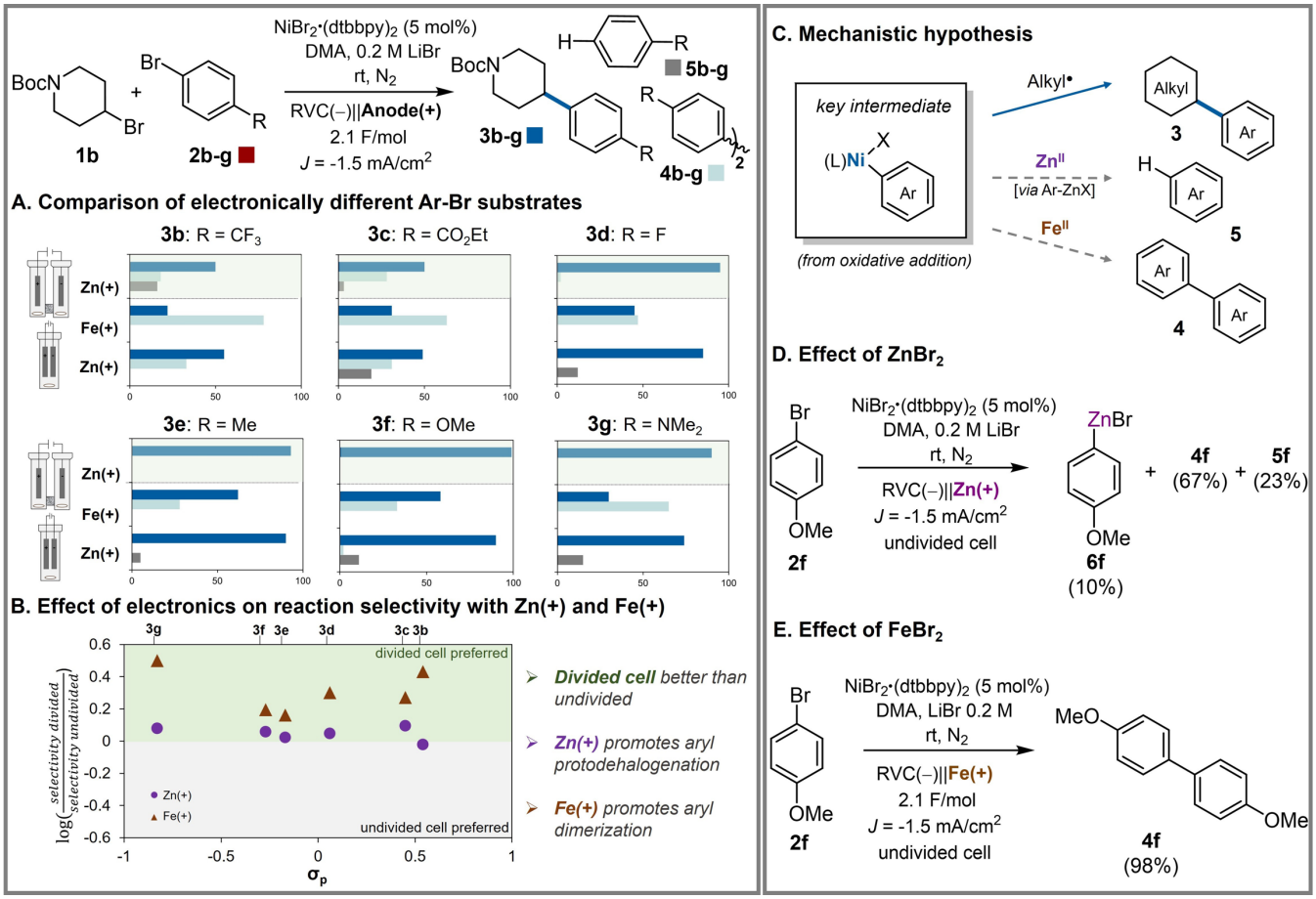

Figure 3. A) Screening of the effect of a divided and undivided cell on various *p*-substituted aryl-Br. Reactions run on 0.5 mmol of **2b-g** with 1.5 equiv of **1b**. B) Plot of log(divided cell selectivity/undivided cell selectivity) vs σ_p. Selectivity defined as [product/(product+side products)]. C) Mechanistic hypotheses about the effect of MX_2 on Ni catalysis. D) Formation of aryl-zinc **6f** using a Zn anode in undivided cell and $NiBr_2$•$(dtbbpy)_2$ (5 mol%) as catalyst. E) Effect of $FeBr_2$ on the homocoupling reaction of **2f**.

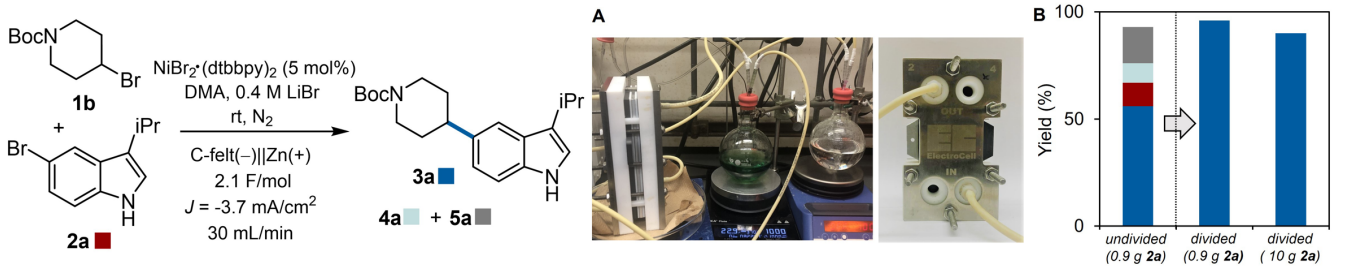

Figure 4. Ni-catalyzed XEC electrolysis of **1b** and **2a** on larger scale using a parallel plate flow reactor with a carbon felt working electrode and Zn counter electrode. A) Photographs of the reaction set-up, showing a side view of the reactor together with the two reservoirs (left) and the front view of the parallel place reactor (right). B) Comparison between results in undivided vs Nafion-115 divided cell on 3.8 mmol **2a** (0.9 g) and performance on 42 mmol **2a** (10 g).

use for different sacrificial anode materials). Therefore, we probed the influence of Zn and Fe anodes on reactions with a series of electronically varied aryl bromides **2b-g** with alkyl bromide **1b.** Each of the reactions was performed in three different ways, in an undivided cell with Zn or Fe as the anode and in a divided cell with a Zn anode (**Figure 3A**). A plot comparing the selectivity in the divided and undivided cell configuration as function of the aryl bromide substituent Hammett parameter (σ_p) shows that nearly all substrates appear in the top half of the plot (**Figure 3B**). These results indicates that use of a divided cell leads to better – often significantly better – performance, including higher yields and selectivity. When side products are observed, proto-dehalogenation of the aryl bromide is typically observed with a Zn anode, while aryl dimerization is favored with an Fe anode.

Ni-catalyzed aryl-alkyl XEC reactions are proposed to proceed through $LNi^{II}(Ar)X$ intermediates (**Figure 3C**).[34,35] The influence of the Zn and Fe anodes can be rationalized by a competition between productive reaction of the $LNi^{II}(Ar)X$ species with an alkyl radical[35,36] versus side reactions promoted by Zn^{2+} or Fe^{2+} ions in solution.

Zn^{2+} ions seem to favor the proto-dehalogenation side product. This observation is rationalized by previous studies showing that aryl groups can undergo Ni-to-Zn transmetalation, forming Zn^{II}-Ar species that are susceptible to protonolysis.[26,37,38] A control experiment was conducted with *p*-methoxyphenyl bromide **2f** to test this hypothesis. Electrolysis of aryl bromide **2f** with $NiBr_2$•$(dtbbpy)_2$ in the absence of the alkyl bromide **1b** generates aryl zinc species **6f** in 10% yield (identified by ^{1}H NMR spectroscopy by comparison to independently prepared **6f**; see Supporting Information, **Figures S20** and **S21**), together with a mixture of side products derived from proto-dehalogenation (**5f**) and biaryl coupling (**4f**).

In contrast, Fe^{2+} ions favor biaryl formation. We are not aware of direct precedents for this observation. Fe salts have been used in cross-electrophile biaryl-coupling reactions with heteroaryl halides;[14,18,39] however, their role in this cases has been attributed to the Lewis acidity of Fe^{2+} preventing inhibition of the Ni-catalyst through coordination of the heteroaryl coupling products. When *p*-methoxyphenyl bromide was subjected to the reaction conditions in the absence of the alkyl bromide **1b** in an undivided cell with a sacrificial Fe anode, the biaryl coupling product **4f** was observed in 98% yield. This result is consistent with preferential formation of biaryl side products from reactions that use an Fe anode. Efforts to probe the origin of this noteworthy observation have been initiated, but control experiments show that the $FeBr_2$ itself is not a competent biaryl coupling catalyst (see Supporting Information, **Figure S22**).

These results have important implications for larger scale applications, prompting us to investigate the role of cell configuration in a parallel-plate flow reactor (**Figure 4A**). The optimized conditions were evaluated in the gram-scale synthesis of **3a** in an undivided parallel-plate reactor (9 cm^2 surface area) equipped with a carbon felt cathode and Zn anode. The reaction led to only 56% yield of **3a**, together with 17% yield of the proto-dehalogenation product **5a** and 9% yield of biaryl **4a**, and 11% of unreacted **2a**. The same reaction was then performed in a reactor equipped with a Nafion-115 membrane separating the anode and cathode. In this case, the reaction afforded **3a** in 96% yield, with no detectable formation of **4a** or **5a** (**Figure 4B**). A similarly favorable outcome was obtained in a larger scale reaction (10 g, 42 mmol **2a**) in a parallel plate reactor with a four-fold higher surface area (36 cm^2, cf. **Figure 4B**; see section 4 in the Supporting Information for details).

Collectively, these results highlight the importance of managing the metal ions derived from sacrificial anodes in electrosynthetic reduction reactions. Examples of deleterious effects of sacrificial anodes are rare,[40–43] and most previous studies in which the role of anode-derive metal ions has been considered highlight beneficial effects.[44–49] For example, Zn^{2+} and Cu^+ ions from Zn and Cu anodes have been used for electrosynthetic preparation of organometallic species,[13,26,27,38,50–52] and Al^{3+} and Fe^{n+} ions derived from Al and Fe anodes participate as Lewis acids in electrosynthetic reductions.[14,29,53–55] In most cases, sacrificial anodes are used for their simplicity and to avoid complications from the use of chemical reductants. The present work demonstrates an important counter example to these beneficial and/or innocent roles of sacrificial anodes, while showing how introduction of a membrane between the anode and cathode compartment provides an effective solution to overcome this problem. This approach highlights a unique opportunity to achieve improved outcomes by using electrochemical, rather than chemical, reduction methods. Chemical Ni-catalyzed XEC reactions commonly use metallic Zn as the source of electrons, but such reactions will necessarily release non-innocent Zn^{2+} ions into solution that can contribute to the formation of side product. Electrochemical XEC reactions may be performed in a divided cell that segregates the Ni-catalyzed reactivity from the reductant, allowing systematic optimization and improved performance of the XEC reaction, without interference from of the source of electrons.

ASSOCIATED CONTENT

Supporting Information

The Supporting Information is available free of charge on the ACS Publications website.

Experimental details with supplemental notes, characterization data, and NMR spectra (PDF)

AUTHOR INFORMATION

Corresponding Author

*Shannon S. Stahl – Department of Chemistry, University of Wisconsin−Madison, Madison, Wisconsin 53706, United States; orcid.org/0000-0002-9000-7665; Email: stahl@chem.wisc.edu

Authors

Luana Cardinale – Department of Chemistry, University of Wisconsin−Madison, Madison, Wisconsin 53706, United States; orcid.org/ 0000-0001-9867-3593.

Gregory L. Beutner – Bristol Myers Squibb, Chemical Process Development, 1 Squibb Drive, New Brunswick NJ 08903, United States; orcid.org/ 0000-0001-8779-1404.

Christopher Y. Bemis – Bristol Myers Squibb, Chemical Process Development, 1 Squibb Drive, New Brunswick NJ 08903, United States; orcid.org/0000-0002-0380-1685.

Daniel J. Weix – Department of Chemistry, University of Wisconsin−Madison, Madison, Wisconsin 53706, United States; orcid.org/0000-0002-9552-3378.

Author Contributions

The manuscript was written through contributions of all authors. All authors have given approval to the final version of the manuscript.

Notes

The authors declare no competing financial interest.

ACKNOWLEDGMENT

The authors thank Dr. McKenna Goetz for helpful discussions and editorial contributions. This research was supported by BMS and the NSF (CHE-2154698). Spectroscopic instrumentation was supported by a generous gift from Paul J. Bender, the NSF (CHE-1048642), and the NIH (S10OD012245).

REFERENCES

(1) Klein, M.; Waldvogel, S. R. Counter Electrode Reactions—Important Stumbling Blocks on the Way to a Working Electro-organic Synthesis. *Angew. Chem. Int. Ed.* **2022**, *61*, e202204140. https://doi.org/10.1002/anie.202204140.

(2) Li, Y.; Wen, L.; Guo, W. A Guide to Organic Electroreduction Using Sacrificial Anodes. *Chem. Soc. Rev.* **2023**, *52*, 1168–1188. https://doi.org/10.1039/D3CS00009E.

(3) Ware, S. D.; Zhang, W.; Guan, W.; Lin, S.; See, K. A. A Guide to Troubleshooting Metal Sacrificial Anodes for Organic Electrosynthesis. *Chem. Sci.* **2024**, 10.1039.D3SC06885D. https://doi.org/10.1039/D3SC06885D.

(4) Chaussard, J.; Folest, J.-C.; Nédélec, J.-Y.; Perichon, J.; Sibille, S.; Troupel, M. Use of Sacrificial Anodes in Electrochemical Functionalization of Organic Halides. *Synthesis* **1990**, *1990*, 369–381. https://doi.org/10.1055/s-1990-26880.

(5) Heard, D. M.; Lennox, A. J. J. Electrode Materials in Modern Organic Electrochemistry. *Angew. Chem. Int. Ed.* **2020**, *59*, 18866–18884. https://doi.org/10.1002/anie.202005745.

(6) Franke, M. C.; Weix, D. J. Recent Advances in Electrochemical, Ni-Catalyzed C−C Bond Formation. *Isr. J. Chem.* **2024**, *64*, e202300089. https://doi.org/10.1002/ijch.202300089.

(7) Su, Z.-M.; Deng, R.; Stahl, S. S. Zinc and Manganese Redox Potentials in Organic Solvents and Their Influence on Nickel-Catalysed Cross-Electrophile Coupling. *Nat. Chem.* **2024**, 1–8. https://doi.org/10.1038/s41557-024-01627-5.

(8) Perkins, R. J.; Hughes, A. J.; Weix, D. J.; Hansen, E. C. Metal-Reductant-Free Electrochemical Nickel-Catalyzed Couplings of Aryl and Alkyl Bromides in Acetonitrile. *Org. Process Res. Dev.* **2019**, *23*, 1746–1751. https://doi.org/10.1021/acs.oprd.9b00232.

(9) Jennings, P. W.; Pillsbury, D. G.; Hall, J. L.; Brice, V. T. Carbon-Carbon Bond Formation via Organometallic Electrochemistry. *J. Org. Chem.* **1976**, *41*, 719–722. https://doi.org/10.1021/jo00866a036.

(10) A summary documenting the number of times metal anodes of different compositions have been used in Ni XEC reactions is provided in section 6 of the Supporting Information.

(11) Meyer, G.; Rollin, Y.; Perichon, J. A Zerovalent Nickel-2,2′-Bipyridine Complex: An Efficient Catalyst for Electrochemical Homocoupling of Ortho-Substituted Halides and Their Heterocoupling with Meta- and Para-Substituted Halides. *J. Organomet. Chem.* **1987**, *333*, 263–267. https://doi.org/10.1016/0022-328X(87)85158-6.

(12) Nédélec, J. Y.; Mouloud, H. A. H.; Folest, J. C.; Perichon, J. Electrochemical Cross-Coupling of Alkyl Halides in the Presence of a Sacrificial Anode. *J. Org. Chem.* **1988**, *53*, 4720–4724. https://doi.org/10.1021/jo00255a011.

(13) Durandetti, S.; Sibille, S.; Perichon, J. Electrochemical Allylation of Carbonyl Compounds Using Nickel Catalyst and Zinc(II) Species. *J. Org. Chem.* **1989**, *54*, 2198–2204. https://doi.org/10.1021/jo00270a033.

(14) Gosmini, C.; Nédélec, J. Y.; Perichon, J. Electrochemical Cross-Coupling between Functionalized Aryl Halides and 2-Chloropyrimidine or 2-Chloropyrazine Catalyzed by Nickel 2,2′-Bipyridine Complex. *Tetrahedron Lett.* **2000**, *41*, 201–203. https://doi.org/10.1016/S0040-4039(99)02037-7.

(15) Sengmany, S.; Léonel, E.; Polissaint, F.; Nédélec, J.-Y.; Pipelier, M.; Thobie-Gautier, C.; Dubreuil, D. Preparation of Functionalized Aryl- and Heteroarylpyridazines by Nickel-Catalyzed Electrochemical Cross-Coupling Reactions. *J. Org. Chem.* **2007**, *72*, 5631–5636. https://doi.org/10.1021/jo070429+.

(16) Oliveira, J. L.; Silva, M. J.; Florêncio, T.; Urgin, K.; Sengmany, S.; Léonel, E.; Nédélec, J.-Y.; Navarro, M. Electrochemical Coupling of Mono and Dihalopyridines Catalyzed by Nickel Complex in Undivided Cell. *Tetrahedron* **2012**, *68*, 2383–2390. https://doi.org/10.1016/j.tet.2012.01.017.

(17) Perkins, R. J.; Pedro, D. J.; Hansen, E. C. Electrochemical Nickel Catalysis for sp^2-sp^3 Cross-Electrophile Coupling Reactions of Unactivated Alkyl Halides. *Org. Lett.* **2017**, *19*, 3755–3758. https://doi.org/10.1021/acs.orglett.7b01598.

(18) Rahil, R.; Sengmany, S.; Le Gall, E.; Léonel, E. Nickel-Catalyzed Electrochemical Reductive Homocouplings of Aryl and Heteroaryl Halides: A Useful Route to Symmetrical Biaryls. *Synthesis* **2018**, *50*, 146–154. https://doi.org/10.1055/s-0036-1589100.

(19) Qiu, H.; Shuai, B.; Wang, Y.-Z.; Liu, D.; Chen, Y.-G.; Gao, P.-S.; Ma, H.-X.; Chen, S.; Mei, T.-S. Enantioselective Ni-Catalyzed Electrochemical Synthesis of Biaryl Atropisomers. *J. Am. Chem. Soc.* **2020**, *142*, 9872–9878. https://doi.org/10.1021/jacs.9b13117.

(20) Jiao, K.; Liu, D.; Ma, H.; Qiu, H.; Fang, P.; Mei, T. Nickel-Catalyzed Electrochemical Reductive Relay Cross-Coupling of Alkyl Halides to Aryl Halides. *Angew. Chem.* **2020**, *132*, 6582–6586. https://doi.org/10.1002/ange.201912753.

(21) Beutner, G. L.; Simmons, E. M.; Ayers, S.; Bemis, C. Y.; Goldfogel, M. J.; Joe, C. L.; Marshall, J.; Wisniewski, S. R. A Process Chemistry Benchmark for sp^2–sp^3 Cross Couplings. *J. Org. Chem.* **2021**, *86*, 10380–10396. https://doi.org/10.1021/acs.joc.1c01073.

(22) Mussari, C. P.; Dodd, D. S.; Sreekantha, R. K.; Pasunoori, L.; Wan, H.; Posy, S. L.; Critton, D.; Ruepp, S.; Subramanian, M.; Watson, A.; Davies, P.; Schieven, G. L.; Salter-Cid, L. M.; Srivastava, R.; Tagore, D. M.; Dudhgaonkar, S.; Poss, M. A.; Carter, P. H.; Dyckman, A. J. Discovery of Potent and Orally Bioavailable Small Molecule Antagonists of Toll-like Receptors 7/8/9 (TLR7/8/9). *ACS Med. Chem. Lett.* **2020**, *11*, 1751–1758. https://doi.org/10.1021/acsmedchemlett.0c00264.

(23) Wheelhouse, K. M. P.; Webster, R. L.; Beutner, G. L. Advances and Applications in Catalysis with Earth-Abundant Metals. *Organometallics* **2023**, *42*, 1677–1679. https://doi.org/10.1021/acs.organomet.3c00292.

(24) Hayler, J. D.; Leahy, D. K.; Simmons, E. M. A Pharmaceutical Industry Perspective on Sustainable Metal Catalysis. *Organometallics* **2019**, *38*, 36–46. https://doi.org/10.1021/acs.organomet.8b00566.

(25) Homodimer yields, based on a maximum dimer yield of 100% **4a**, correspond to a 0.5:1 molar ratio of **4a**:**2a**.

(26) Klein, P.; Lechner, V. D.; Schimmel, T.; Hintermann, L. Generation of Organozinc Reagents by Nickel Diazadiene Complex Catalyzed Zinc Insertion into Aryl Sulfonates. *Chem. – Eur. J.* **2020**, *26*, 176–180. https://doi.org/10.1002/chem.201904545.

(27) Gosmini, C.; Rollin, Y.; Nédélec, J. Y.; Perichon, J. New Efficient Preparation of Arylzinc Compounds from Aryl Halides Using Cobalt Catalysis and Sacrificial Anode Process. *J. Org. Chem.* **2000**, *65*, 6024–6026. https://doi.org/10.1021/jo000459b.

(28) Day, C. S.; Somerville, R. J.; Martin, R. Deciphering the Dichotomy Exerted by Zn(II) in the Catalytic sp^2 C–O Bond Functionalization of Aryl Esters at the Molecular Level. *Nat. Catal.* **2021**, *4*, 124–133. https://doi.org/10.1038/s41929-020-00560-3.

(29) Kumar, G. S.; Zhu, C.; Kancherla, R.; Shinde, P. S.; Rueping, M. Metal Cations from Sacrificial Anodes Act as a Lewis Acid Co-Catalyst in Electrochemical Cross-Coupling of Aryl Bromides and Aziridines. *ACS Catal.* **2023**, *13*, 8813–8820. https://doi.org/10.1021/acscatal.3c01503.

(30) Previous studies of this reaction indicated that proto-dehalogenation of **2a** can arise from β-hydride elimination from a Ni-alkyl intermediate; however, the observations here suggest protonolysis of an arylzinc intermediate is the primary origin of the hydrogen atom.

(31) Franke, M. C.; Longley, V. R.; Rafiee, M.; Stahl, S. S.; Hansen, E. C.; Weix, D. J. Zinc-Free, Scalable Reductive Cross-Electrophile Coupling Driven by Electrochemistry in an Undivided Cell. *ACS*

Catal. **2022**, *12*, 12617–12626. https://doi.org/10.1021/acscatal.2c03033.

(32) Li, H.; Breen, C. P.; Seo, H.; Jamison, T. F.; Fang, Y.-Q.; Bio, M. M. Ni-Catalyzed Electrochemical Decarboxylative C–C Couplings in Batch and Continuous Flow. *Org. Lett.* **2018**, *20*, 1338–1341. https://doi.org/10.1021/acs.orglett.8b00070.

(33) The formation of Fe^{2+} rather than Fe^{3+} from the anodic oxidation of an Fe rod under our experimental conditions was established through various OCP measurements, see figure **S23** in the Supporting Information.

(34) Weix, D. J. Methods and Mechanisms for Cross-Electrophile Coupling of Csp^2 Halides with Alkyl Electrophiles. *Acc. Chem. Res.* **2015**, *48*, 1767–1775. https://doi.org/10.1021/acs.accounts.5b00057.

(35) Biswas, S.; Weix, D. J. Mechanism and Selectivity in Nickel-Catalyzed Cross-Electrophile Coupling of Aryl Halides with Alkyl Halides. *J. Am. Chem. Soc.* **2013**, *135*, 16192–16197. https://doi.org/10.1021/ja407589e.

(36) Lin, Q.; Spielvogel, E. H.; Diao, T. Carbon-Centered Radical Capture at Nickel(II) Complexes: Spectroscopic Evidence, Rates, and Selectivity. *Chem* **2023**, *9*, 1295–1308. https://doi.org/10.1016/j.chempr.2023.02.010.

(37) Gilbert, M. M.; Trenerry, M. J.; Longley, V. R.; Castro, A. J.; Berry, J. F.; Weix, D. J. Ligand–Metal Cooperation Enables Net Ring-Opening C–C Activation/Difunctionalization of Cyclopropyl Ketones. *ACS Catal.* **2023**, *13*, 11277–11290. https://doi.org/10.1021/acscatal.3c02643.

(38) Sibille, S.; Ratovelomanana, V.; Périchon, J. Electrochemical Conversion of Functionalised Aryl Chlorides and Bromides to Arylzinc Species. *J Chem Soc Chem Commun* **1992**, No. 3, 283–284. https://doi.org/10.1039/C39920000283.

(39) Urgin, K.; Barhdadi, R.; Condon, S.; Léonel, E.; Pipelier, M.; Blot, V.; Thobie-Gautier, C.; Dubreuil, D. Some Mechanistic Aspects of a Nickel-Catalyzed Electrochemical Cross-Coupling between Aryl Halides and Substituted Chloropyridazines. *Electrochimica Acta* **2010**, *55*, 4495–4500. https://doi.org/10.1016/j.electacta.2010.02.092.

(40) Yousef, U. S. Electroinitiated Cationic Polymerization of P-Chloromethyl Styrene Using Different Sacrificial Anode Materials in Nitromethane. *Eur. Polym. J.* **1998**, *34*, 637–643. https://doi.org/10.1016/S0014-3057(97)00201-2.

(41) Lorandi, F.; Fantin, M.; Isse, A. A.; Gennaro, A. Electrochemically Mediated Atom Transfer Radical Polymerization of N-Butyl Acrylate on Non-Platinum Cathodes. *Polym. Chem.* **2016**, *7*, 5357–5365. https://doi.org/10.1039/C6PY01032F.

(42) Peters, B. K.; Rodriguez, K. X.; Reisberg, S. H.; Beil, S. B.; Hickey, D. P.; Kawamata, Y.; Collins, M.; Starr, J.; Chen, L.; Udyavara, S.; Klunder, K.; Gorey, T. J.; Anderson, S. L.; Neurock, M.; Minteer, S. D.; Baran, P. S. Scalable and Safe Synthetic Organic Electroreduction Inspired by Li-Ion Battery Chemistry. *Science* **2019**, *363*, 838–845. https://doi.org/10.1126/science.aav5606.

(43) Luo, J.; Chavez, M.; Durante, C.; Gennaro, A.; Isse, A. A.; Fantin, M. Improvement of Electrochemically Mediated Atom Transfer Radical Polymerization: Use of Aluminum as a Sacrificial Anode in Water. *Electrochimica Acta* **2022**, *432*, 141183. https://doi.org/10.1016/j.electacta.2022.141183.

(44) Silvestri, G.; Gambino, S.; Filardo, G.; Greco, G.; Gulotta, A. Electrochemical Carboxylation of Benzal Chloride. *Tetrahedron Lett.* **1984**, *25*, 4307–4308. https://doi.org/10.1016/S0040-4039(01)81424-6.

(45) Sahloul, K.; Sun, L.; Requet, A.; Chahine, Y.; Mellah, M. A Samarium "Soluble" Anode: A New Source of SmI_2 Reagent for Electrosynthetic Application. *Chem. – Eur. J.* **2012**, *18*, 11205–11209. https://doi.org/10.1002/chem.201201390.

(46) Sun, L.; Sahloul, K.; Mellah, M. Use of Electrochemistry to Provide Efficient SmI_2 Catalytic System for Coupling Reactions. *ACS Catal.* **2013**, *3*, 2568–2573. https://doi.org/10.1021/cs400587s.

(47) Sun, L.; Mellah, M. Efficient Electrosynthesis of $SmCl_2$, $SmBr_2$, and $Sm(OTf)_2$ from a "Sacrificial" Samarium Anode: Effect of n-Bu_4NPF_6 on the Reactivity. *Organometallics* **2014**, *33*, 4625–4628. https://doi.org/10.1021/om500222a.

(48) Matthessen, R.; Fransaer, J.; Binnemans, K.; Vos, D. E. D. Electrocarboxylation: Towards Sustainable and Efficient Synthesis of Valuable Carboxylic Acids. *Beilstein J. Org. Chem.* **2014**, *10*, 2484–2500. https://doi.org/10.3762/bjoc.10.260.

(49) Lu, L.; Siu, J. C.; Lai, Y.; Lin, S. An Electroreductive Approach to Radical Silylation via the Activation of Strong Si–Cl Bond. *J. Am. Chem. Soc.* **2020**, *142*, 21272–21278. https://doi.org/10.1021/jacs.0c10899.

(50) Chapman, M. R.; Shafi, Y. M.; Kapur, N.; Nguyen, B. N.; Willans, C. E. Electrochemical Flow-Reactor for Expedient Synthesis of Copper–N-Heterocyclic Carbene Complexes. *Chem. Commun.* **2015**, *51*, 1282–1284. https://doi.org/10.1039/C4CC08874C.

(51) Nicholls, T. P.; Bourne, R. A.; Nguyen, B. N.; Kapur, N.; Willans, Charlotte. E. On-Demand Electrochemical Synthesis of Tetrakisacetonitrile Copper(I) Triflate and Its Application in the Aerobic Oxidation of Alcohols. *Inorg. Chem.* **2021**, *60*, 6976–6980. https://doi.org/10.1021/acs.inorgchem.1c00488.

(52) Wang, M.; Zhang, C.; Ci, C.; Jiang, H.; Dixneuf, Pierre. H.; Zhang, M. Room Temperature Construction of Vicinal Amino Alcohols via Electroreductive Cross-Coupling of *N*-Heteroarenes and Carbonyls. *J. Am. Chem. Soc.* **2023**, *145*, 10967–10973. https://doi.org/10.1021/jacs.3c02776.

(53) Gosmini, C.; Lasry, S.; Nedelec, J.-Y.; Perichon, J. Electrochemical Cross-Coupling between 2-Halopyridines and Aryl or Heteroaryl Halides Catalysed by Nickel-2,2′-Bipyridine Complexes. *Tetrahedron* **1998**, *54*, 1289–1298. https://doi.org/10.1016/S0040-4020(97)10225-3.

(54) Ribeiro, R. T.; De Mattos, I. L.; Sengmany, S.; Barhdadi, R.; Léonel, E.; Cachet-Vivier, C.; Navarro, M. Iron Role in the Electrochemical Cyclopropanation Reaction of Activated Olefins and Halogenated Compounds. *Electrochimica Acta* **2011**, *56*, 7352–7360. https://doi.org/10.1016/j.electacta.2011.06.029.

(55) Manabe, S.; Wong, C. M.; Sevov, C. S. Direct and Scalable Electroreduction of Triphenylphosphine Oxide to Triphenylphosphine. *J. Am. Chem. Soc.* **2020**, *142*, 3024–3031. https://doi.org/10.1021/jacs.9b12112.

TOC Graphic

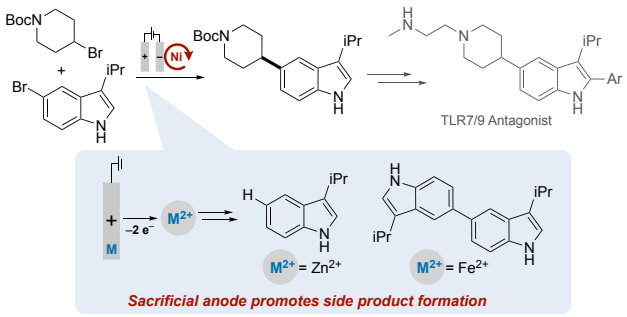
BocN
Br
Br
iPr
Ni
BocN
iPr
TLR7/9 Antagonist
iPr
Ar
M
−2 e⁻
M2+
iPr
M2+ = Zn2+
iPr
M2+ = Fe2+
Sacrificial anode promotes side product formation